ISSN 0018-151X, High Temperature, 2020, Vol. 58, No. 6, pp. 812–817. © Pleiades Publishing, Ltd., 2020.
Russian Text © The Author(s), 2020, published in Teplofizika Vysokikh Temperatur, 2020, Vol. 58, No. 6, pp. 876–882.

THERMOPHYSICAL PROPERTIES OF MATERIALS

Influence of Thermal Effects on the Transport Characteristics of Cellulose Acetate Porous Films

S. I. Lazarev[a], Yu. M. Golovin[a], S. V. Kovalev[a], D. S. Lazarev[a, *], and A. A. Levin[a]

[a] *Tambov State Technical University (FSBEI HE "TSTU"), Tambov, 392000 Russia*

**e-mail: geometry@mail.nnn.tstu.ru*

Received October 21, 2019; revised March 25, 2020; accepted June 18, 2020

Abstract—Experimental data have been obtained, and the characteristics of the moisture content and permeability of cellulose acetate porous materials were analyzed via thermal action. Dynamic thermogravimetric analysis found that the destruction process in an air-dry sample of the membrane begins at 21°C. It is accompanied by a 2% weight loss and an endothermic effect. The destruction ends at 50°C. With a subsequent increase in temperature, the manifestation of endothermic effect continues a temperature of 120–175°C with the maximum rate of mass loss at 146°C. The weight loss ends at about 190°C and is 6.5%. The study of MGA-80 and MGA-95 porous cellulose acetate films at transmembrane pressure upon temperature exposure showed that the permeability and specific output flow to water increase as the temperature rises to 50°C. Analysis of dependences of the specific output flow on temperature revealed that the specific output flow to water increases by ~18% upon an initial temperature rise of 10°C. This is due to structural changes in the cellulose acetate layer. A further increase in temperature by 15°C leads to an increase in permeability by ~10%. These phenomena are associated with the process of structural transformation in the active layer and the polymer substrate of the MGA-95 and MGA-80P membranes, respectively.

DOI: 10.1134/S0018151X20060139

INTRODUCTION

Questions about the effect of temperature on the transport characteristics of membrane materials, which affect the kinetics of mass and heat transfer, remain highly controversial [1–20]. It was noted [1] that there is an increase in the limiting diffusion current density and a decrease in the length of the plateau current–voltage characteristics (CVCs) after the heat treatment of a strongly acidic sulfonic-cation exchange membrane characterized by low catalytic activity in the water dissociation reaction and by a high thermal stability of fixed groups due to an increase in the fraction of the conducting surface and the development of the membrane microrelief. In [2], the membranes were studied in temperature conditions with molecular dynamics, which made it possible to calculate the diffusion coefficients of Lennard-Jones fluids in the membrane and to obtain the dependences of the diffusion coefficients on the temperature, density, and mixture composition.

The operation of polymer films at elevated temperatures [3, 4] and in intense current modes [5] allows a significant increase in their mass-transfer characteristics [6] and, hence, the efficiency of electrodialysis processes. A molecular-statistical method was developed [7] to model the pervaporation process on hybrid silicon oxide membranes, which demonstrated membrane selectivity to water, and it was also determined that the flow of components exponentially depends on the pore size and temperature. It was established [8] via scanning electron microscopy that an increase in macroporosity, the appearance of new structural defects, and a decrease in the fraction of the ion-exchange phase on the membrane surface occur as a result of prolonged exposure to elevated temperatures. It was found [9] that membrane surface properties such as electrical and geometric inhomogeneity determine the intensity of electroconvective mixing of a solution at the interface and the parameters of diffusion layers in the MK-40 sulfonic-cation exchange membrane after chemical conditioning and thermal action at current densities exceeding the limiting diffusional values. The correlation between changes in the morphology and the degree of membrane-surface hydrophobicity was noted in [10]. As a result of prolonged membrane thermostating at temperatures above room temperature, the degree of hydrophobicity decreases due to a significant increase in the size of cavities and cracks.

Studies were carried out on a thermogravimetric analyzer of epoxy composites with various reinforcing fillers in [11]. The study of the kinetics of thermal transformation of samples showed that materials made of composites reinforced with fabrics are the most promising for use in technological processes. Shrimp chitin and chitosan with various degrees of deacetylation by thermogravimetric analysis were studied in [12]. It was noted that the temperature at which the

decomposition rate of the studied samples is maximal is 290–295°C and does not depend on the degree of sample deacetylation. The rate of weight loss of samples at 290–295°C is due to the degree of deacetylation. The thermal imidization of polyamide acid and a polymer with a molecular imprint based on it were studied in [13]. It was established that the dehydration process takes place in three stages. The polymer film forms in the second stage of the second step and then undergoes high-temperature dehydrocyclization (the third stage at $T = 453$ K), during which the process of water detaching (elimination) with the formation of imide bonds takes place, as well as the removal of solvent residues from the product.

The effect of the solution temperature, salinity, and solution circulation rate on the permeate flow and the content of dissolved substances was estimated in [14]. It was noted that the lifetime and productivity of the membrane depend on a number of factors (concentration polarization, sedimentation). A special factor in the study of membranes is the polymer sensitivity to temperature effects in the processing of solutions at a temperature of 20–40°C, which causes an increase in permeability up to 60%, both in the presence and in the absence of solutes in the liquid. Studies [15, 16] showed that research on direct osmosis is attracting a lot of attention to wastewater treatment, desalination of salt sea water, and power generation. The study of the influence of a working solution temperature of 20–45°C on the laboratory separation unit of direct osmosis showed that a higher temperature provides high performance characteristics, greater water extraction, and high concentration coefficients, which is associated with improved mass transfer in the near-membrane boundary layer. However, a higher temperature causes adverse effects on membrane cleaning. It was shown [17] how the effect of temperature on the direct osmosis system initiates a high permeability of the solvent and solute, which is associated with a change in the thermodynamic properties of solutions and the manifestation of various polarization phenomena.

The kinetics of crystallization processes and phase transformations in the ZhS6U alloy was studied via thermal analysis [18]. It is shown that the modification leads to a change in the melt structure and crystallization conditions, as well as the release of the main and excess phases. These changes consist of a decrease in the crystallization interval of the alloy due to a decrease in the liquidus temperature and an increase in the growth rate of the solid phase in the initial period of crystallization. The influence of membrane orientation, the rate of solution to be separated, the solution temperature, and the combined effect of both temperature and solution rate on the membrane permeability were studied in [19] in order to increase the productivity of the direct-osmosis process. It was shown [20] that low thermal efficiency and productivity with water are one of the main problems hindering the commercialization of the membrane-distillation process. The authors found that the phenomenon of inversion of the total water productivity, which was confirmed with two different mathematical models and demonstrated experimentally, takes place in connection with a decrease in the flow of water vapor through the membrane, as well as an increase in heat loss due to thermal conductivity with an increase in the geometric dimensions of the membrane.

Analysis of the literature data [1–20] shows the influence of temperature effects on the moisture content and permeability characteristics of other polymer membrane materials, e.g., cellulose acetate films, must be studied with more informative physical methods. This will make it possible to explain and predict the mechanism of mass and heat transfer of substances and to develop equations for a theoretical calculation of the transport characteristics in the surface layer and pore space of polymer film materials [21, 22]. The goal of this work is to study the thermal effect on the transport characteristics of porous, cellulose, acetate films.

EXPERIMENTAL

An EXSTAR TG/DTA 7200 thermogravimetric analyzer (Japan) was used for the study. The curves of the thermal mass loss (TG), differential thermal mass loss (DTG), and differential thermal analysis (DTA) were recorded at a rate of 5°C/min in the range from 16°C to 200°C.

The experimental setup described in detail in [23] was used to study the permeability. The permeability coefficient was calculated based on experimental data according to the following dependence:

$$\alpha = \frac{V}{F_m \tau P},$$

where V is the volume of collected permeate, m^3; F_m is the area of the working surface of the film of a rectangular sample, m^2; τ is the time of the experiment, s; and P is the transmembrane pressure, MPa.

Samples of commercially available MGA-80 and MGA-95 cellulose acetate films were used in the experiments. One was stored in a closed container of an air-dry medium, and the other was placed in an aqueous medium (distilled water) for 3 h for water absorption at room temperature. Table 1 shows the characteristics of cellulose acetate porous membranes.

RESULTS AND DISCUSSION

The thermogravimetric analysis data in Fig. 1 made it possible to determine the total moisture content of the cellulose acetate film and the degree of its filling with water. The data make it possible to find the differences between membranes that differ in their chemical structure and the structure formed from macromolecules. Thermoanalytical curves that describe the process of membrane dehydration for air-dry and water-saturated samples of membranes were obtained.

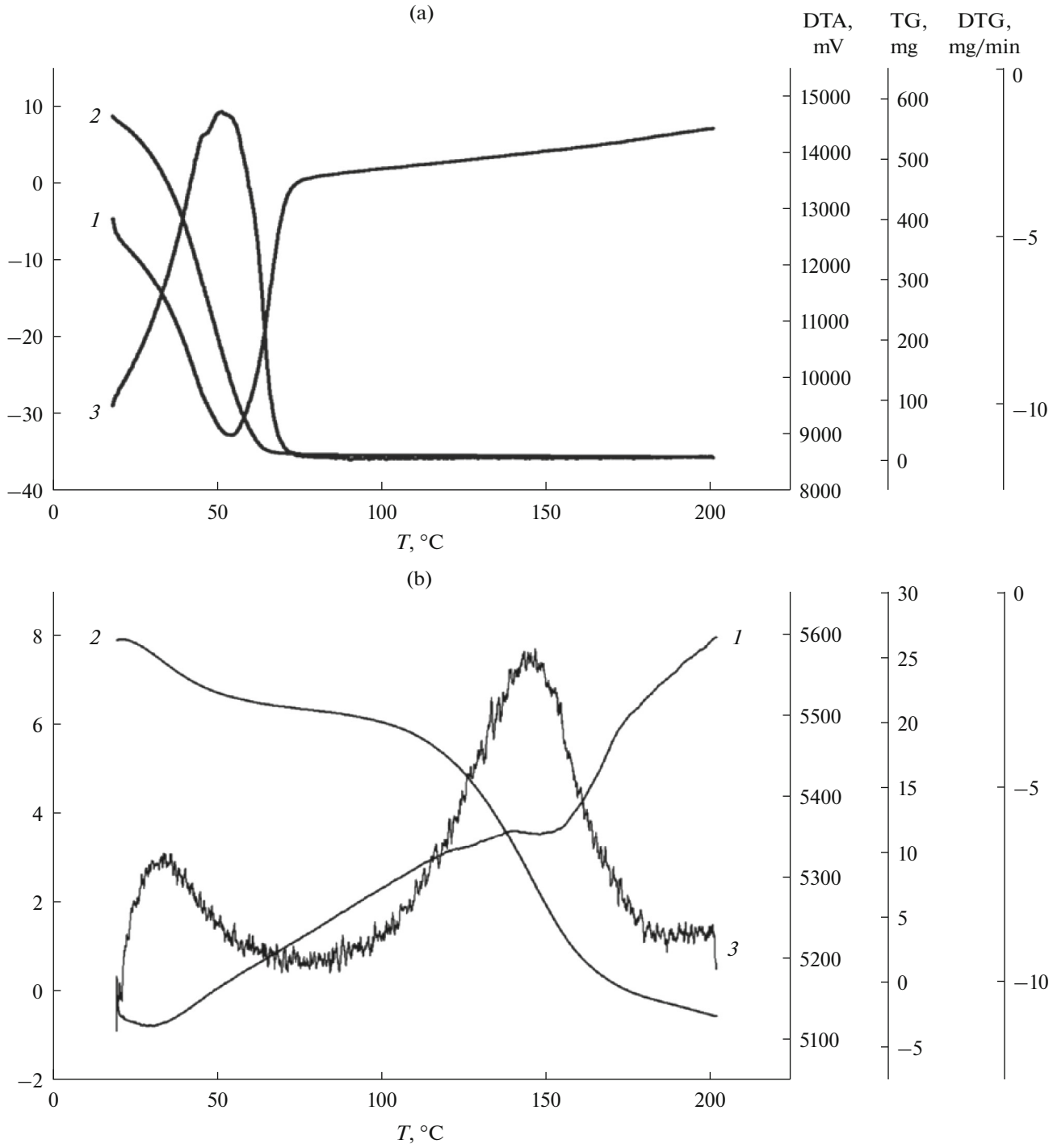

Fig. 1. Curves of dynamic thermogravimetric analysis of cellulose acetate film MGA-95: (a) water-saturated sample, (b) air-dry sample; (*1*) DTA curve, (*2*) TG, (*3*) DTG.

For the studied samples of cellulose acetate films with different moisture contents at temperatures of 21–200°C, the DTA curves showed an endothermic effect accompanied by a change in the mass on the TG curves, which corresponded to the removal of the solvent from the porous film phase. The thermogravimetric curves in $\alpha-T$ coordinates plotted by the dehydration of air-dry and water-saturated membrane samples are S shaped, which confirms the complex nature of the interaction of the solvent (water) with the membrane and suggests different rates of solvent release at different stages of dehydration [24].

To better understand and establish the temperature range and the amount of removed solvent, the differ-

Table 1. Performance characteristics of MGA-80P and MGA-95 cellulose acetate films

Parameters	MGA-95	MGA-80P
Transmembrane pressure, MPa	5.0	
Minimum productivity to filtrate at 25°C, $m^3/(m^2\ s)$	9.16×10^{-6}	1.75×10^{-5}
Retention coefficient to 0.15% NaCl, not less	0.95	0.80
Working pH range	3–8	
Maximum temperature, °C	50	

ential DTA curve and weight loss curves with a linear increase in temperature were recorded. It was found that the destruction process begins at 21°C in an air-dry sample. It ends at 50°C with a 2% weight loss and an endothermic effect. With a subsequent increase in temperature from 120 to 175°C, the endothermic effect continues with a maximum rate of weight loss at 146°C. At about 190°C, the weight loss stops with a value of 6.5%.

It is likely that the sorbed moisture in this temperature range is removed from the surface, but the most important thing is the process of destruction of nonequilibrium hydrogen bonds with the release of water.

An absolutely amazing picture is observed in a water-saturated membrane sample (Fig. 1b). The beginning of weight loss occurs at 21°C, ends at about

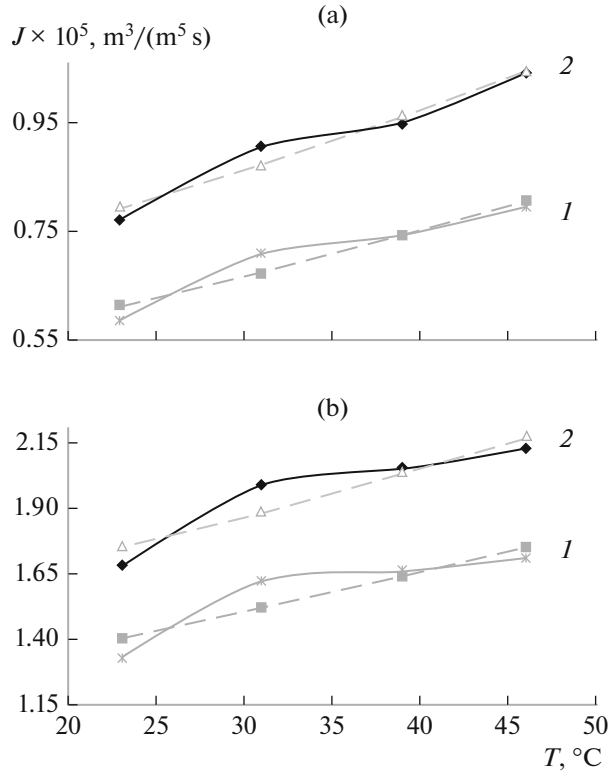

Fig. 2. Dependence of the specific output flow for MGA-95 (a) and MGA-80P (b) cellulose acetate films on the thermal effect and transmembrane pressure: (*1*) $P = 3$ MPa; (*2*) 4.

65°C with a maximum rate at 51°C, and is 42% with a total moisture capacity of 70% or more. The process occurs with one endothermic effect from 20°C to 65°C. Note that easily removable water molecules at low temperatures are located on the outer surfaces of the membrane pores and do not form hydrogen bonds. However, 28% of water remains in the sample—the water that participates in the formation of a structured nematic phase with the formation of a hydration shell. The destruction of this hydration shell occurs at a temperature of 125–175°C. The removal of moisture from the film surface and from its pores is probably related to the structure and type of cellulose mixtures, as observed in [25, 26]. For example, it was noted [26] that the thermograms of cellulose acetate films and their copolymer mixtures have several stages of weight loss. In this case, for a water-saturated sample (Fig. 1b), the weight loss occurs in two stages (curve *3*) due to the removal of adsorbed moisture at a temperature of 50–200°C due to the extensive degradation of cellulose acetate (an area of significant moisture loss).

Analysis of the data—the dependences of the specific output flux on the temperature effect and transmembrane pressure (Fig. 2, curves *1* and *2*)—allows us to note that, upon an increase in temperature, the specific output flux in a small interval increases sharply for both the MGA-95 and MGA -80P cellulose acetate films and then monotonically increases up to 45°C, as evidenced by a smoother slope of the permeability curve in the direction of increasing. Transmembrane pressure is the driving force of the baromembrane process; therefore, the productivity of the membrane separation process by water increases with an increase in transmembrane pressure.

The values of the permeability of the studied porous, cellulose, acetate films due to thermal action at the selected range of temperature variation differ from each other (Table 2). This probably indicates a difference in the structure of the active layer and substrates of films (membrane), the pore diameter, and the shape in the surface (active) layer and pore (interfiber) space of the substrate. The pores have different shapes and form the sorption space of the membrane, which is probably larger for the MGA-80P membrane than for the MGA-95 membrane. Quantitative analysis of membrane permeability to water shows that it is higher in the MGA-80P membrane than in the MGA-95

Table 2. Dependence of permeability on the temperature and transmembrane pressure for MGA-95, and MGA-80P membranes at $\tau = 900$ s

Membrane	T, °C	P, MPa	$\alpha \times 10^5$, $m^3/(m^2\ s\ MPa)$	$\alpha_{calc} \times 10^5$, $m^3/(m^2\ s\ MPa)$	m	n	d, %
MGA-95	22	3.0	0.195	0.203	1.054	3.717	−4.27
	30		0.236	0.225			4.84
	38		0.248	0.247			0.23
	45		0.265	0.269			−1.42
	22	4.0	0.193	0.198	1.026	3.730	−2.61
	30		0.227	0.219			3.60
	38		0.239	0.241			−0.90
	45		0.261	0.262			−0.40
MGA-80P	22	3.0	0.446	0.471	1.119	2.886	−5.60
	30		0.541	0.509			5.95
	38		0.556	0.548			1.34
	45		0.570	0.585			−2.62
	22	4.0	0.421	0.438	1.041	2.814	−4.12
	30		0.496	0.473			4.71
	38		0.512	0.509			0.66
	45		0.532	0.541			−1.78

d is the deviation of the experimental values of water permeability from the values calculated with formula (2).

membrane. This is due to the high rate of water absorption by the membrane material, i.e., a greater capacity for water sorption by the MGA-80P membrane. The water sorption by the MGA-95 and MGA-80P membranes most likely changes the supramolecular structure of the crystalline phase and decreases the size of the coherent scattering region and crystallinity. The structure of the drainage layer of the amorphous phase changes at the molecular and supramolecular levels. Presumably, an interfacial layer forms due to the interaction of the polar groups NH and COO- of contacting polymers. Water, acting as a plasticizer, structures the cellulose acetate macromolecules in the interfacial layer of the film due to the hydration of polar groups of macromolecules [27, 28].

To summarize, it can be noted that curves 1 and 2 (Fig. 2) of the specific output flow and the given data on permeability (Table 2) illustrate the process of an increase in the specific output flow with respect to the increase in the thermal action, all other things being equal for the studied partitions. Analysis of the dependences of the specific output flow on temperature showed that an increase in the specific output flow to water by ~18% is observed upon an initial temperature increase by 10°C. This is due to structural changes in the cellulose acetate layer. A further 15°C increase in temperature leads to a smaller increase in permeability, ~10%. Such phenomena are associated with the process of structural transformation in the active layer and the polymer substrate of the MGA-95 and MGA-80P membranes, respectively.

The described change in permeability is probably associated with the dependence of the change in flux on the nanoscopic parameters of membranes (pores, defects), as well as the difference in the thickness of the active layer of the MGA-95 and MGA-80P membranes. It should be borne in mind that the drainage layer of MGA-80P and MGA-95 cellulose acetate membranes is made of nonwoven lavsan and polypropylene.

As can be seen from the data in Fig. 2 and Table 2, the kinetic process of a change in the specific output flux and permeability from thermal action and transmembrane pressure is described by the function [29, 30]

$$\alpha_{calc} = \frac{J_{calc}}{P}, \quad J_{calc} = m\alpha_0 P\left(\frac{T_0}{T}\right)^n, \qquad (1)$$

where α_0 is the permeability to distilled water at 22°C, $m^3/(m^2\ s\ MPa)$; m and n are the empirical coefficients; and T_0 and T are the initial and current solution temperatures, °C.

The values of the empirical coefficients m and n and other calculated parameters for equation (1) are given in Table 2.

CONCLUSIONS

As a result of the performed experimental and theoretical studies on the thermogravimetric analysis of air-dry and water-saturated samples and the effect of temperature on the permeability of cellulose acetate porous films, the following conclusions can be drawn.

1. The obtained data from thermogravimetric analysis make it possible to establish both the total moisture content and the degree of porous-film filling with moisture. Here, it becomes possible to identify differences among films differing in moisture content both on the surface and in the pore space. Thermoanalyti-

cal curves describing the process of membrane dehydration were obtained for each film sample. For all studied samples of porous films with different moisture contents at temperatures of 21–200°C, the curves of differential thermal analysis showed an endothermic effect accompanied by a change in weight on the curves of thermal weight loss, which corresponds to the removal of the solvent from the phase of the porous film.

2. Analysis of the dependences of the specific output flow on temperature found that the specific output flow to water increases by ~18% upon an initial temperature increase of 10°C, and the permeability increases by ~10% with a further increase in temperature by 15°C. A mathematical expression was proposed and the values of empirical coefficients were calculated for an analytical description of the permeability, the specific output flow in the kinetic process of liquid-phase processing at varying temperatures, and the transmembrane pressure for the studied cellulose acetate porous films.

FUNDING

This work was supported by the Russian Foundation for Basic Research, project no. 19-38-90117.

REFERENCES

1. Vasil'eva, V.I., Akberova, E.M., and Zabolotskii, V.I., *Russ. J. Electrochem.*, 2017, vol. 53, no. 4, p. 398.
2. Anashkin, I.P., Klinov, A.V., and Anashkina, A.V., *Vestn. Kazan. Tekhnol. Univ.*, 2017, vol. 20, no. 22, p. 48.
3. Smagin, V.N., Zhurov, N.N., Yaroshevsky, D.A., and Yevdokimov, O.Y., *Desalination*, 1983, vol. 46, nos. 1–3, p. 253.
4. Onuki, K., Hwang, G.J., and Arifal Shimizu, S., *J. Membr. Sci.*, 2001, vol. 192, nos. 1–2, p. 193.
5. Pourcelly, G., Nikonenko, V.V., Pismenskaya, N.D., and Yaroslavtsev, A.V., in *Ionic Interactions in Natural and Synthetic Macromolecules*, Hoboken, NJ: Wiley, 2012, p. 761.
6. Pis'menskaya, N.D., Nikonenko, V.V., Mel'nik, N.A., Pourcelli, G., and Larchet, K., *Russ. J. Electrochem.*, 2012, vol. 48, no. 6, p. 610.
7. Klinov, A.V., Anashkin, I.P., and Akberov, R.R., *High Temp.*, 2018, vol. 56, no. 1, p. 70.
8. Akberova, E.M., Yatsev, A.M., Kozhukhova, E.Yu., and Vasil'eva, V.I., *Kondens. Sredy Mezhfaznye Granitsy*, 2017, vol. 19, no. 2, p. 158.
9. Akberova, E.M., *Kondens. Sredy Mezhfaznye Granitsy*, 2017, vol. 19, no. 3, p. 314.
10. Vasil'eva, V.I., Pismenskaya, N.D., Akberova, E.M., and Nebavskaya, K.A., *Russ. J. Phys. Chem. A*, 2014, vol. 88, nos. 7–8, p. 1293.
11. Shustov, I.I., Koitov, S.A., and Mel'nikov, V.N., *Vestn. Samarsk. Gos. Aerokosm. Univ.*, 2014, no. 1(43), p. 181.
12. Kuchina, Yu.A., Dolgopyatova, N.V., Novikov, V.Yu., Konovalova, I.N., Printseva, M.Yu., and Sagaidachnyi, V.A., *Vestn. Murmansk. Gos. Tekh. Univ.*, 2015, no. 1, p. 94.
13. Semiletova, E.S., Zyablov, A.N., and Selemenev, V.F., *Sorbtsionnye Khromatogr. Protsessy*, 2012, vol. 12, no. 5, p. 734.
14. Goosen, M.F.A., Sablani, S.S., Al-Maskari, S.S., Al-Belushi, R.H., and Wilf, M., *Desalination*, 2002, vol. 144, nos. 1–3, p. 367.
15. Zhao, S. and Zou, L., *Desalination*, 2011, vol. 278, nos. 1–3, p. 157.
16. You, S.-J., Wang, X.-H., Zhong, M., Zhong, Y.-J., Yu, C., and Ren, N.-Q., *Chem. Eng. J.*, 2012, vols. 198–199, p. 52.
17. Phuntsho, S., Vigneswaran, S., Kandasamy, J., Hong, S., Lee, S., and Shon, H.K., *J. Membr. Sci.*, 2012, vols. 415–416, p. 734.
18. Eremin, E.N., Filippov, Yu.O., Minnekhanov, G.N., and Lopaev, B.E., *Omsk. Nauchn. Vestn.*, 2013, no. 1(117), p. 63.
19. Hawari, Al.H., Kamal, N., and Altaee, A., *Desalination*, 2016, vol. 398, p. 98.
20. Lee, J.-G., Alsaadi, A.S., Karam, A.M., Francis, L., Soukane, S., and Ghaffour, N., *J. Membr. Sci.*, 2017, vol. 544, p. 126.
21. Bushman, A.V., Lomonosov, I.V., Fortov, V.E., and Khishchenko, K.V., *Khim. Fiz.*, 1994, vol. 13, no. 1, p. 64.
22. Bushman, A.V., Lomonosov, I.V., Fortov, V.E., and Khishchenko, K.V., *Khim. Fiz.*, 1994, vol. 13, no. 5, p. 97.
23. Lazarev, S.I., Lazarev, K.S., Kovaleva, O.A., Kazakov, V.G., and Strel'nikov, A.E., *Izv. Vyssh. Uchebn. Zaved., Khim. Khim. Tekhnol.*, 2017, vol. 60. Vyp. 5, p. 74.
24. Kotova, D.L. and Selemenev, V.F., *Termicheskii analiz ionoobmennykh materialov* (Thermal Analysis of Ion-Exchange Materials), Moscow: Nauka, 2002.
25. Zavastin, D. Cretescu, I., Bezdadea, M., Bourceanu, M., Drăgan, M., Lisa, G., Mangalagiu, I., Vasić, V., and Savić, J., *Colloids Surf., A*, 2010, vol. 370, nos. 1–3, p. 120.
26. Kamal, H., Abd-Elrahim, F.M. and Lotfy, S., *J. Radiat. Res. Appl. Sci.*, 2014, vol. 7, no. 2, p. 146.
27. Lazarev, S.I., Golovin, Yu.M., Kovalev, S.V., and Lazarev, D.S., *High Temp.*, 2019, vol. 57, no. 5, p. 641.
28. Mel'nikova, G.B., Zhavnerko, G.K., Chizhik, S.A., and Bil'dyukevich, A.V., *Pet. Chem.*, 2016, vol. 56, p. 406.
29. Lazarev, S.I., Golovin, Yu.M., Khorokhorina, I.V., Kovalev, S.V., and Levin, A.A., *Izv. Vyssh. Uchebn. Zaved., Khim. Khim. Tekhnol.*, 2019, vol. 62, no. 10, p. 89.
30. Deryagin B.V., Churaev, N.V., and Muller, V.M., *Poverhnostnye sily* (Surface Forces), Moscow: Nauka, 1985.

Translated by V. Selikhanovich